ΣΥΝΕΔΡΙΑ ΤΗΣ 10ΗΣ ΑΠΡΙΛΙΟΥ 1997

ΠΡΟΕΔΡΙΑ ΝΙΚΟΛΑΟΥ ΜΑΤΣΑΝΙΩΤΗ

ΦΥΣΙΚΗ. — **Climatology of the solar erythemal UV in Athens, Greece,** by *H. T. Mantis, Corresponding Member of the Academy of Athens and C. C. Repapis C. M. Philandras, A. G. Paliatsos, C. S. Zerefos, A. F. Bais, C. Meleti and D. S. Balis**.

ABSTRACT

Three years of observations of the erythemally active component of solar radiation using the Yankee Environmental Systems Pyranometer are analysed to provide a climatological description of the UV exposure levels and their variability in the urban Mediterranean environment. Contributions made by column ozone and cloud cover to the observed fluctuations in UV are estimated in separate analyses. During the warmer months there appears to be a substantial reduction of the solar UV by atmospheric components other than ozone, a conclusion that is supported by comparison of the observations with the predictions of radiative transfer models and with the UV observations in a rural mid latitude environment (McKenzie et al., 1991).

1. INTRODUCTION

The stimulus for the present study and numerous other studies of the solar ultraviolet climate has been the observation of a recent decline in stratospheric ozone and the possibility of biological damage that may follow a continued decrease in the UV absorption by this atmospheric component. The solar beam is depteted in passing through the atmosphere by absorption and backscattering by various gaseous components and by aerosols and cloud

* Ο. ΜΑΝΤΗΣ, Χ. Κ. ΡΕΠΑΠΗΣ, Κ. Μ. ΦΙΛΑΝΔΡΑΣ, Α. Κ. ΠΑΛΙΑΤΣΟΣ, Χ. Σ. ΖΕΡΕΦΟΣ, Λ. Φ. ΜΠΑΗΣ, Χ. ΜΕΛΕΤΗ καὶ Δ. Σ. ΜΠΑΛΗΣ, **Κλιματολογία τῆς ἡλιακῆς ὑπεριώδους ἀκτινοβολίας στὴν Ἀθήνα.**

particles. For the biologically active UVB band (280-320 nm) which contains only 1.7% of the incoming solar irradiance, depletion by ozone absorption and molecular backscatter is generally greater than 80% and can approach 100% under heavy cloud cover. Both ozone and cloud cover, the atmospheric componenets which dominate UV depletion, have a variation over wide range of spatial and temporal scales (Ambach and Blumthaler, 1994; Prasad et al., 1992). The detection of a significant secular change in the UV level may therefore require a long period of accurate UV measurements for different climatic regimes. It is the purpose of this study to first summarize the principal features of the UV climate in an urban eastern Mediterranean setting, in an analysis of UV measurements in central Athens. And secondly, to estimate the relative contributions of column ozone and cloud cover in the determination of the UV climate.

2. DATA

a. Ultraviolet observations

Continuous UV measurements are made from the rooftop of the Academy of Athens Research Centre (Alt. 95 m, Lat. 37.996^0 N, Long. 23.732^0 E) using the Yankee Environmental Systems (YES) pyranometer, model UVB-1, recording averages of irradiance at 10 minute intervals. The UV irradiance and daily dose are reported as erythemal effective radiation, EER in the notation adopted by Forster (1995), to indicate that the spectral irradiance is weighted by the erythemal action spectrum of McKinley and Diffey (1987). Although the pyranometer has a spectral response approximating the erythemal weighting function, the spectral absorption cross section of ozone in the UVB region varies by more than two orders of magnitude and therefore the pyranometer output is not linearly proportional to EER but varies with solar elevation (Appendix A Figs. A1, A2). The manufacturer supplies a computer program for converting the pyranometer signal to erythemal effective irradiance using a radiative transfer model developed by Green et al. (1974).

Figure 1 shows the time series of daily EER dose for the period 13 April 1993 to 31 December 1995. The dominant feature is the large annual variation following the change in solar zenith angle. The relative variation of EER from winter to summer is three times that for total solar radiation at midlatitudes. While EER fluctuations from day to day and at other intraannual

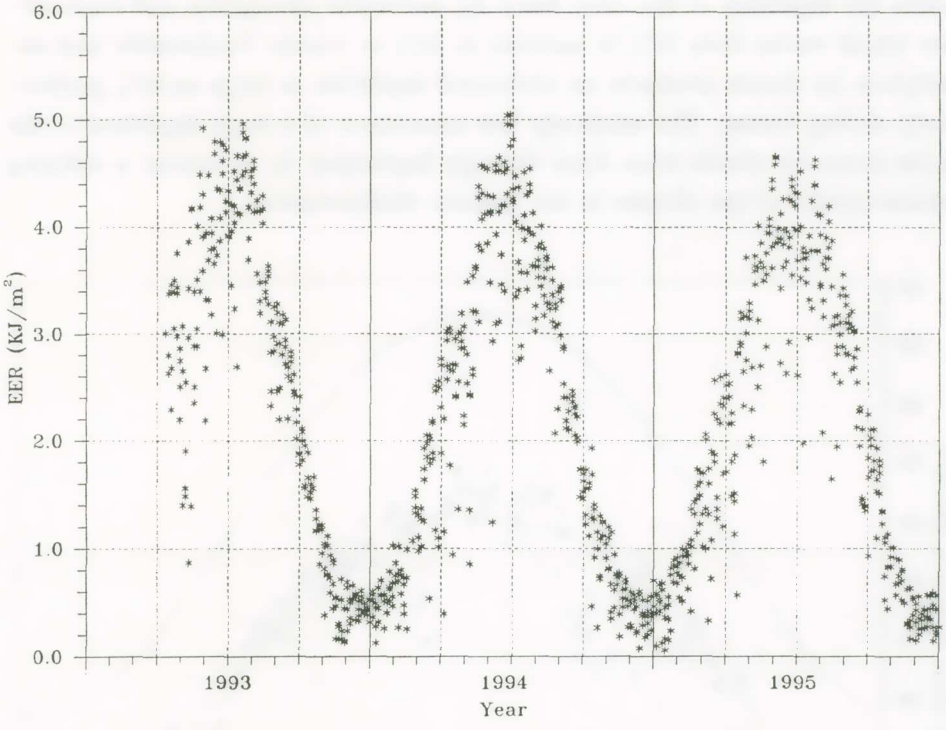

Fig. 1. Time series of daily EER dose for Athens, KJ /m², 13 Apr. 1993 - 31 Dec. 1995.

time scales are large, the annual course of EER dose in 1994 and 1995 are similar and the correlation of monthly mean values is quite high (r= 0.995). A summary of statistics of the UV Climate is given in Appendix B.

b. Solar radiation and clouds

Eppley pyranometer observations of solar total and diffuse radiation as well as observations of the standard meteorological parameters are made at the National Observatory of Athens (NOA, Alt. 107 m, Lat. 37.972° N, Long. 23.718° E) located ~3 km southwest of the site of the UV measurements. The data for the time series of daily values of total solar radiation for 1994 shown in Figure 2 were taken from the Climatological Bulletin published by the Institute. The smooth curve represents the solar radiation received at the top of the atmosphere. The difference between an envelope enclosing the observations and the curve for radiation received at the top of the atmosphere repre-

sents the depletion of the solar beam by molecular absorption and backscatter which varies from 24% in summer to 33% in winter. Backscatter and absorption by clouds produces an additional depletion as large as 60% particularly during winter. The relatively low occurrence of a large depletion of the solar beam by clouds from June through September is, of course, a defining characteristic of the climate in the Eastern Mediterranean.

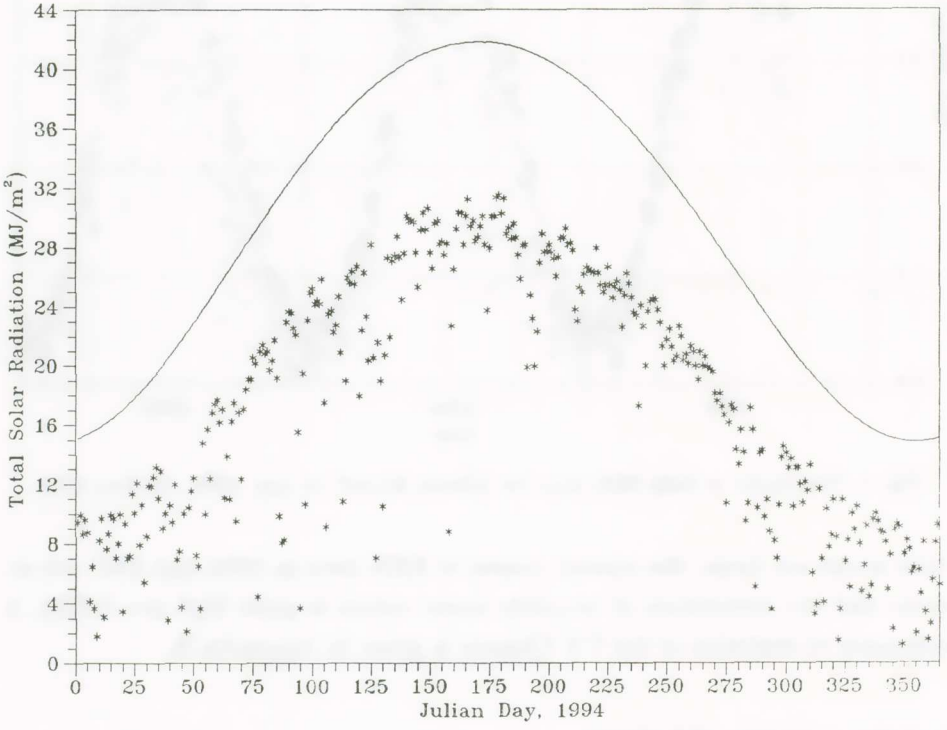

Fig. 2. Time series of daily total solar radiation (MJ /m² day) for Athens 1994. The smooth curve represents total solar radiation received at the top of the atmosphere (Athens latitude).

c. Ozone

Daily observations of ozone column using the Dobson instrument are made at the Laboratory of Meteorology of the University of Athens located less than 2 km to the south of the UV measurements. A time series of daily values of total ozone for 1994 is shown in Figure 3; the data were taken from the WMO publication Ozone Data for the World. The smooth curve represents

the annual course of ozone as determined by a polynomial of third degree. While there is a pronounced annual component with a maximum in April and a minimum in November, the day to day variability is very large, particularly in late winter and spring. The annual curve which varies by 64 DU or 20% from maximum to minimum, accounts for only 30% of the daily variance. Climatological summaries of ozone observations are also presented in Appendix B.

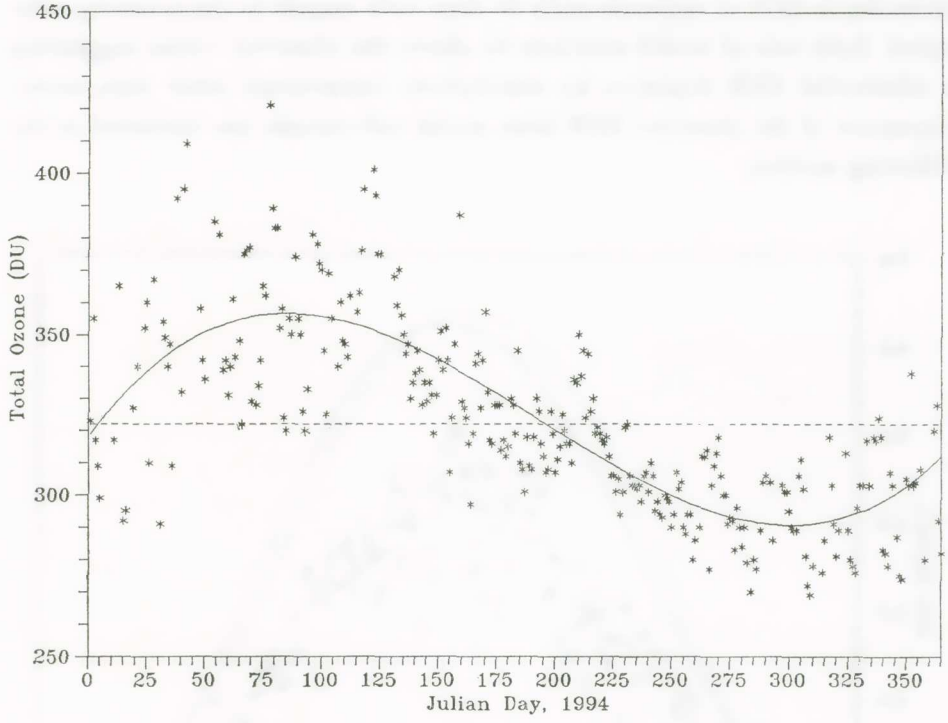

Fig. 3. Time series of daily Dobson measurements of total ozone (DU) in central Athens for 1994. The smooth curve gives the annual variation determined by a polynomial fit.

ANALYSIS

a. EER response to the seasonal variation of ozone column

To provide a reference for the seasonal change in EER dose to be expected with a seasonally varying ozone column of plus or minus 10%, a series of calculations were made using a radiative transfer model computer program, UV-

CALC, supplied by Yankee Environmental Systems. The radiative transfer model is adapted from one developed by Green et al. (1974). Calculations of EER were made at twice monthly intervals assuming clear skies, average aerosol load and for two sets of total ozone: a constant ozone column of 323 DU, the annual average value, and for an annually varying ozone column given by the polynomial fit. Both sets of solutions are shown as smooth curves in Figure 4 along with a replot of the time series of EER observations for 1994. The major effect of the annual variation in column ozone is to produce a phase lag in EER of approximately 20 days with respect to the incoming solar signal. Both sets of model solutions lie above the observed values suggesting a substantial EER depletion by atmospheric components other than ozone. Departure of the observed EER from model calculations are discussed in the following section.

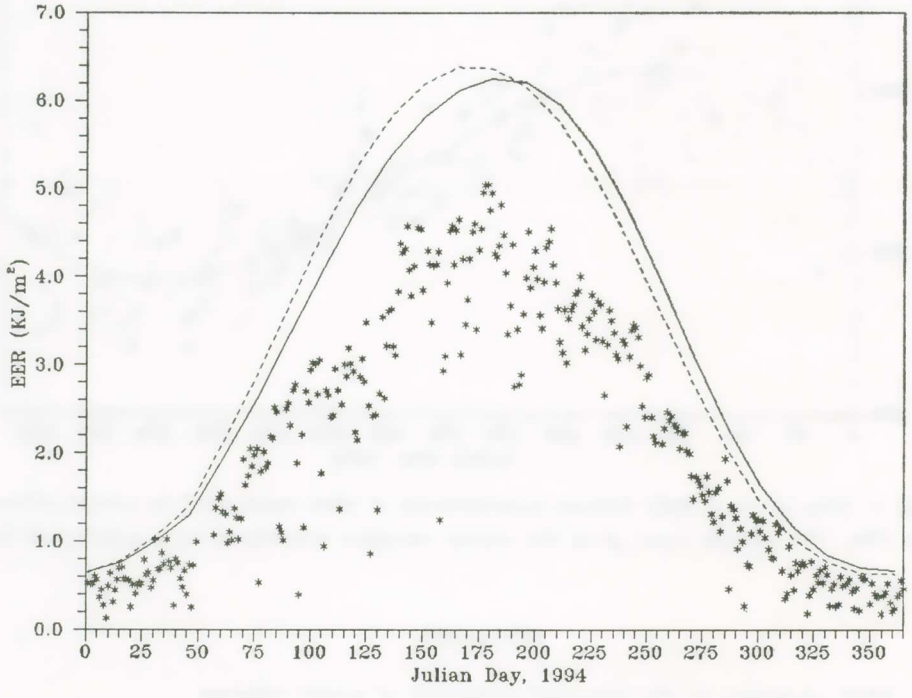

Fig. 4. Time series of daily measurements of EER dose (KJ /m².day) in central Athens for 1994. The smooth curves give model calculations of clear sky irradiance assuming a constant column ozone of 323 DU (broken line) and column ozone varying annually as given by a polynomial fit (solid line).

b. EER depletion by clouds

Lacking a quantitative measure of the optical depth of clouds the transmission of total solar radiation is assumed as surrogate. The transmission of total solar radiation is defined as $T_t = S_t/S_0$ where S_0 is the daily value of incoming total solar radiation (smooth curve, Fig. 2) and S_t the observed total solar radiation. The relative transmission of EER dose T_r is defined by the ratio E_r/E_c where E_r is the observed EER dose and E_c is the EER dose calculated for clear skies and annually varying total ozone (smooth curve, Fig. 4).

Because of the large variation in cloud cover from winter to summer as well as a seasonal variation in UV depletion by coponents other than ozone the comparison of T_r with T_t is presented in two scatter diagrams: the warmer half year (arbitrarily set, 1 April to 30 September) and colder half year. Scatter diagrams of T_r versus T_t for 1994 are shown in Figs. 5a, b with the line of best fit. The correlations of T_r with T_t are almost identical for both pe-

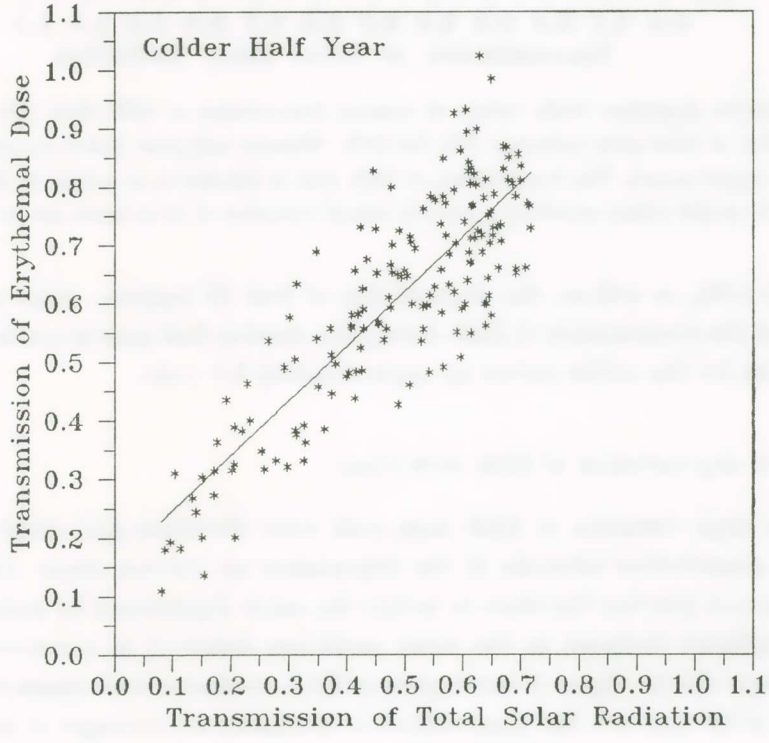

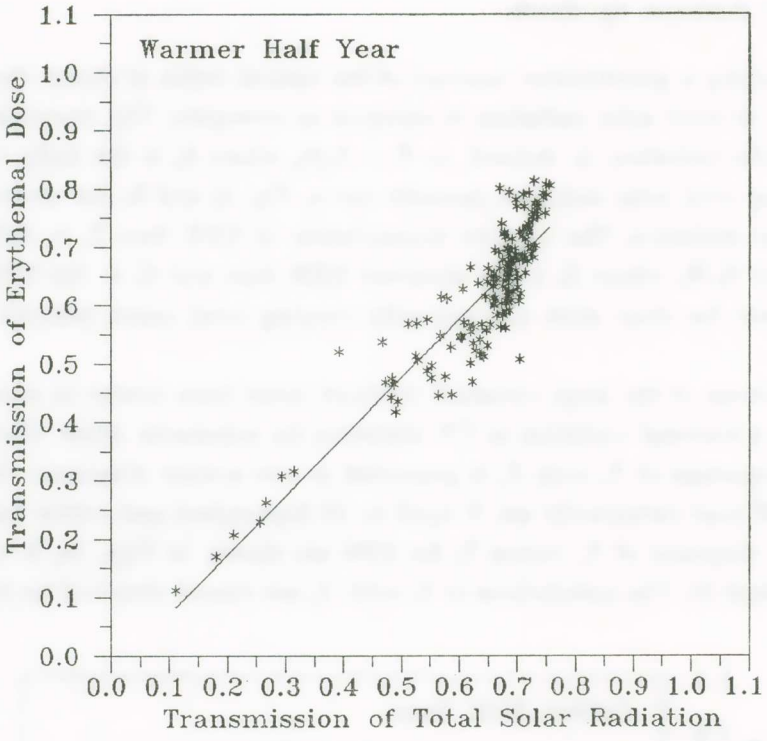

Fig. 5. Scatter diagrams: Daily values of relative transmission of EER dose (Tr) versus transmission of total solar radiation (Tt) for 1994. Warmer half year (lower panel) colder half year (upper panel). The transmission of EER dose is calculated as a ratio of observed EER to model values assuming a smooth annual variation of total ozone (see text).

riods (r$\rangle$ 0.88), as well as, the slope of line of best fit (approx. slope of 1.0). Note that the transmission of EER during the warmer half year is consistently lower than for the colder period by approximately 0.1 units.

c. Day to day variation of EER with ozone

The large variation of EER dose with solar elevation and cloud cover make a quantitative estimate of the dependence on column ozone difficult. It is common practice therefore to isolate the ozone dependence by examining EER irradiance (reduced to the mean earth-sun distance) at constant solar zenith angle (SZA). Figure 6 shows plots of EER irradiance with ozone column for SZA of 63^0 and 45^0. The observations of irradiance are averages of AM and

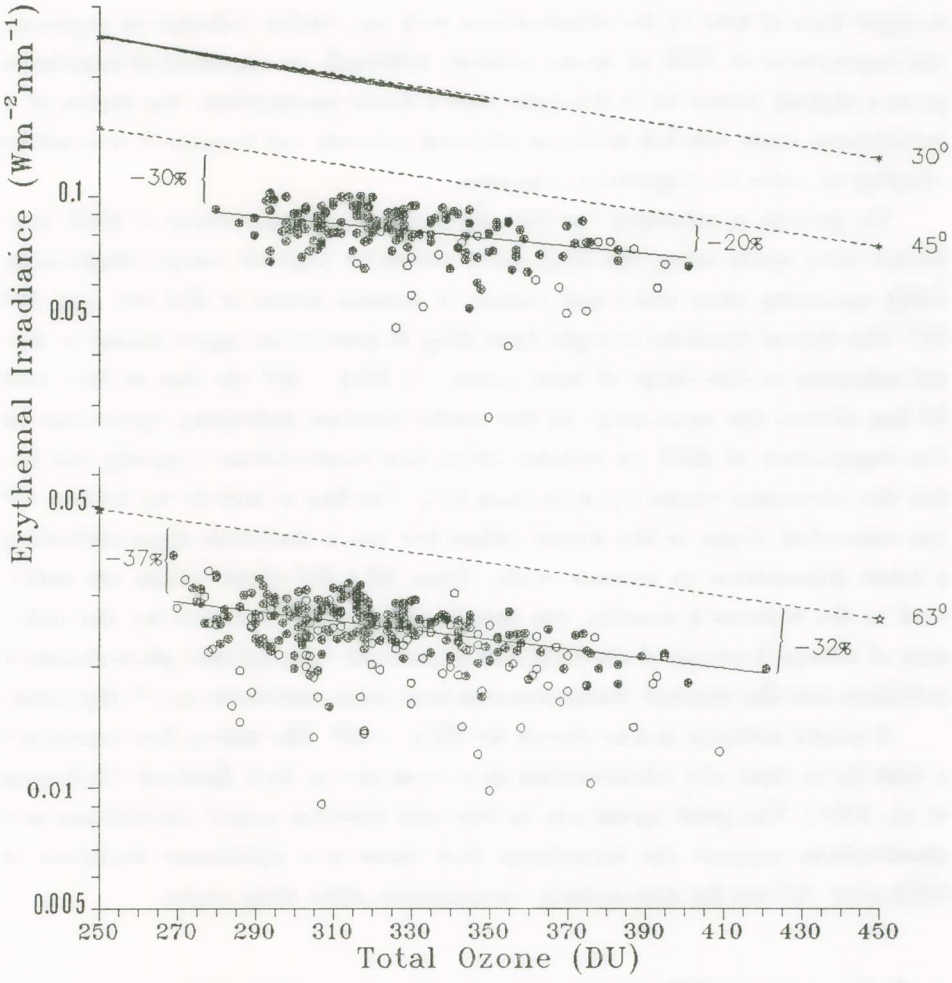

Fig. 6. Scatter diagram for EER irradiance at constant SZA (W/m²) versus total ozone (DU) for 1994. SZA = 45° upper panel and SZA = 63° lower panel. Solid circles indicate EER observations made during an hour when sun was visible and the straight lines through the data show an exponential best fit to these data. The straight lines above the data represent the boundary of clear sky polutions for EER irradiance. The dotted line at SZA = 30° represents the boundary for clear sky observations at a rural midlatitude (see text).

PM readings in part to avoid a diurnal bias in comparison with ozone measurements usually made near midday. Solid circles indicate irradiance observations made during an hour that Campbell-Stokes instrument recorded the so-

lar disk visible. Note that irradiance is plotted on a logarithmic scale and straight lines of best fit for observations with sun visible indicate an exponential dependence of EER on ozone column. Although an exponential depedence gives a slightly better fit to the data than a linear assumption, the choice of a logarithmic scale was not made on physical grounds but because it is a better display of order of magnitude relations.

To provide a reference for the observations, computations of EER irradiance were made using the Madronich radiative transfer model (Madronich, 1989) assuming clear skies and values of column ozone of 250 DU and 450 DU. The dotted (broken) straight lines (Fig. 6) provide an upper bound to model solutions in this range of total ozone. At SZA = 63° the line of data best fit has almost the same slope as the model solution indicating agreement on the dependence of EER on column ozone but observations typically fall below the calculated values by more than 30%. The line of best fit for SZA = 45° lies somewhat closer to the model values but has a shallower slope indicating a lesser dependence on column ozone. Since SZA 45° observations are restricted to the warmer 8 months, the sample distribution is biased by the inclusion of a large fraction of observations when both tropospheric photochemical pollution and the summer Mediterranean haze may contribute to UV depletion.

A model solution is also shown for SZA = 30°. The heavy line represents a best fit to clear sky observations at a rural site in New Zealand (McKenzie et al., 1991). The good agreement in this case between model calculations and observations support the hypothesis that there is a significant depletion of EER over Athens by atmospheric components other than ozone.

d. Daily course of EER irradiance under clear skies; illustrative examples

Five days with high values of transmission of total solar radiation and with continuous sunshine as measured by the Campbell-Stokes recorder were selected to illustrate the magnitude of day to day changes in EER both that due to changes in total ozone and that produced by fluctuations of other atmospheric components. Figures 7a, b show the daily course of EER irradiance on two successive days in March following the passage of a cyclonic disturbance and a subsequent decrease of 8% in ozone column from 421 DU to 389 DU. EER observations are entered at 10 minute intervals. The smooth curve represents the Madronich radiative transfer model solutions for these values

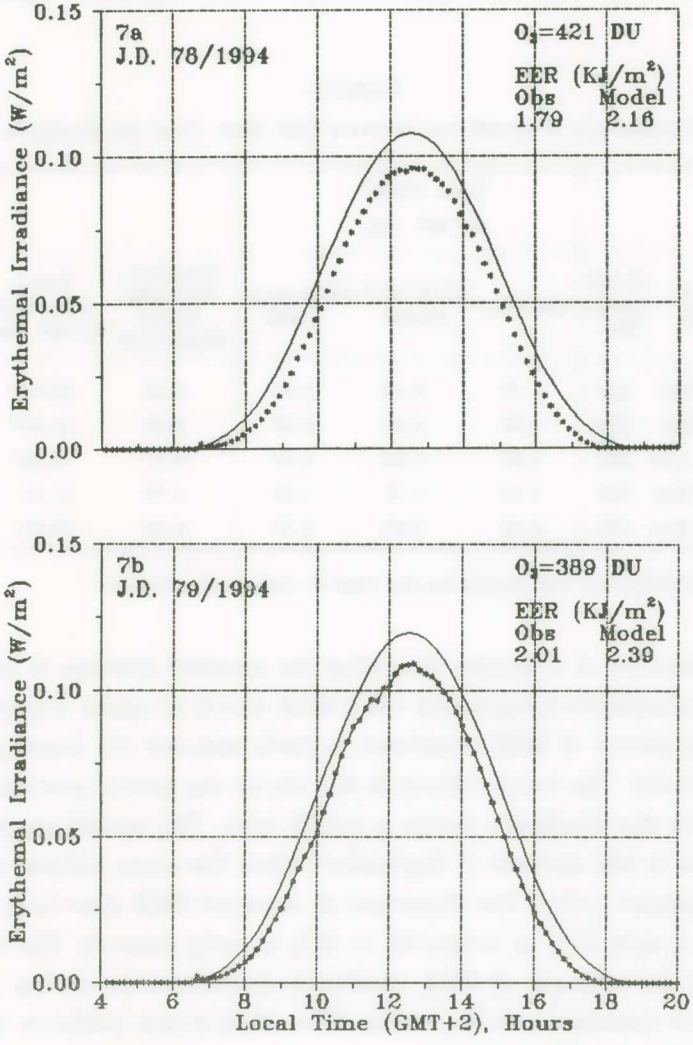

Fig. 7. Daily course of EER irradiance for two successive days 19 and 20 March 1994 with little cloudiness and an 8% decrease in ozone column. The smooth curves show the Madronich model solution for clear skies, total ozone of 421 DU (Fig. 7a) and 389 DU (Fig. 7b).

of total ozone assuming clear skies, a stratospheric aerosol of optical depth 0.38, and a surface albedo of 0.03. Both observed and model prediction of EER dose increase by 11% in response to the 8% decrease in total ozone. The observed dose, however, is 16% below the model predictions on both days.

These data along with total solar radiation observations are summarized in Table 1.

TABLE 1

Comparison of model and observed EER dose. Clear sky examples.

Julian Day	Date 1994	Total Ozone DU	EER DOSE KJ/m². day			Fraction: EER obs/ Model Madronich	Total Solar Rad KJ/m². day	Tt, Transmission Total Solar Rad
			Observed	UV-CALC Model	Madronich Model			
78	19 Mar	421	1.79	2.19	2.16	0.83	20.97*	0.708
79	20 Mar	389	2.01	2.47	2.39	0.84	21.39*	0.716
166	15 Jun	341	4.65	6.00	5.32	0.87	31.26*	0.748
244	1 Sep	298	3.45	4.74	4.36	0.79	24.50	0.719
257	14 Sep	294	2.11	4.02	3.77	0.56	20.36	0.649

* Total Solar radiation was maximum for year to date of observation.

The next set of examples illustrates the seasonal increase in depletion of EER by atmospheric components other than clouds or ozone. Figure 8a shows the diurnal course of EER irradiance in early summer (15 June) just before solar maximum. The ozone column is still above the annual average; and maximum clear sky irradiance occurs a month later. The second graph (Fig. 8b) is for a case in late summer (1 September) when the ozone column approaches annual minimum value. The departure of observed EER dose from the model prediction is now 21% as compared to 13% in early summer. The final graph (Fig. 8c) is an example of EER irradiance measurements during an Athens air pollution episode on 14 September 1994. This severe pollution episode occurred during the MEDCAPHOT campaign of intensive study of photochemical pollution in the eastern Mediterranean. Data from aircraft measurements of concentrations of various pollutants as well as ground based observations are available on computer diskettes (Ziomas, 1997).

Clouds are not a factor causing the large departures in EER irrandiance from model calculations seen in the Figure 8c (Ref. to Table 1). The National Observatory recorded an average cloud cover of zero on 14 September (less than 0.3 octals) the only such observation during summer 1994. There is even a short interval near 10 : 00 hrs, the time when solar radiation increases most

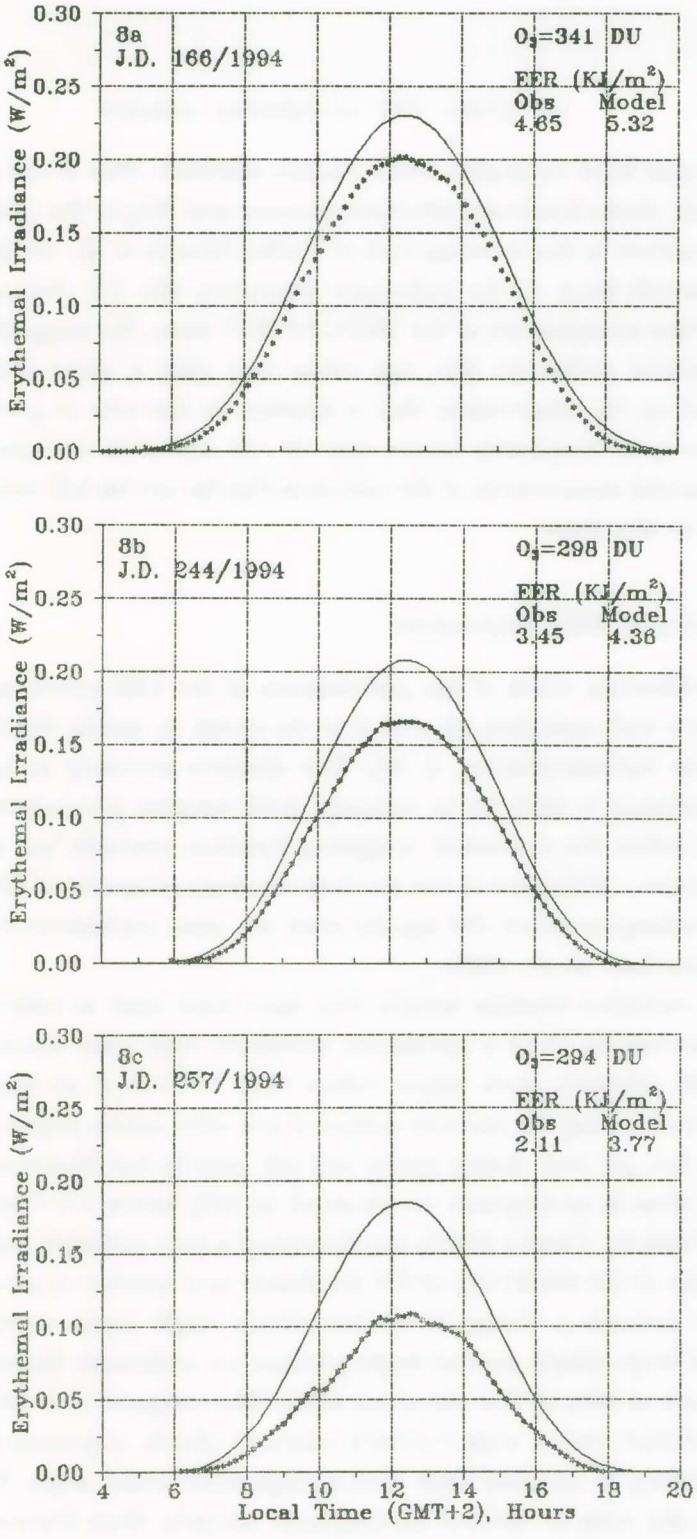

Fig. 8. Daily course of EER irradiance for 15 June 1994 (Fig. 8a) for 1 September 1994 (Fig. 8b) and for 14 September 1994 (Fig. 8c). The smooth curves show the Madronich model solution for clear skies and observed total ozone.

rapidly, that EER irradiance levels remain constant. This is also the time of most rapid photochemical production of ozone and NO_2 in the mixture of pollutants emitted in the morning rush of traffic (Mantis et al., 1992). A quantitative identification of the pollutants producing this UV depletion will require further examination of the MEDCAPHOT data. The suggestion that the photochemical pollutants NO_2 and ozone may play a major role is further supported by the observation that a decrease in the rate of growth of EER irradiance quite frequently occurs near 10 : 00 AM even on days of low pollution. Careful examination of the curves in Figs 8a and 8b will reveal a change in slope at this hour.

e. Accuracy of EER observations

A calibration check of the performance of the YES pyranometer after a year and a half operation showed it to be stable to within the limits of the calibration instrumentation, $\pm$ 5%. The absolute accuracy at low levels of EER irradiance is difficult to estimate both because pyranometer response does not follow the erythemal weighting function precisely but also because there remains a difference in the absolute accuracy estimates of EER irradiance at wavelengths below 300 nm for even the most sophisticated instrumentation (Gardiner et al., 1993).

The radiative transfer models that have been used as reference for the EER observations show a systematic difference with solar zenith angle. The Madronich solutions have larger values than UV-CALC at large SZA but lesser values during the summer season of low solar zenith angles. They agree within a few per cent during spring and fall months but Madronich solutions for EER dose in midsummer are as much as 10% below UV-CALC (see Fig. 8a and Table 1). Forster (1995) has developed a new radiative transfer model for a study of the sensitivity of UV irradiance to a number of parameters and finds for example a change in surface albedo might cause change of 7% in EER and tropospheric aerosol could produce an additional depletion of EER by as much as 50% of that for ozone alone. The comparison of the Madronich and UV-CALC values with Forster's solutions (Table 2) provide an estimate of uncertainty in modeled EER dose at high solar zenith angle. Solutions are for clear sky with or without stratospheric aerosols. Only Forster specifies a surface albedo of 0.2. Note that for winter for 200 DU at 52^0 N latitude there

TABLE 2

EER Dose, Comarison of Radiative Transfer Solutions of Clear Sky Examples

OZONE DU	AEROSOLS	FORSTER	UV-CALC	MADRONICH
		SUMMER 52° Lat		
350	YES	4.72	4.86	4.40
	NO	5.02	5.67	—
250	YES	—	7.05	6.54
	NO	—	8.22	—
200	YES	9.49	8.67	—
	NO	—	10.19	—
		WINTER 52° Lat		
350	YES	—	0.103	—
	NO	0.161	0.115	—
200	YES	—	0.176	0.312
	NO	0.259	0.191	0.341
		WINTER 38° Lat		
322	YES	—	0.615	0.756

is a very large percentual difference in UV-CALC and Madronich solutions while Forster's value falls in between.

4. CONCLUSIONS

The response in EER irradiance to variation in column ozone is of the same order as that derived from radiative transfer models. On average, however, EER irradiance is at least 20% below that for clear skies. The transmission of EER dose is well correlated with the transmission of total solar radiation and day to day variations in EER dose are more dependent on variations in cloud cover than variations in ozone column (Fig. 5 and statistics, Appendix B). Summer values of EER dose, even under clear skies, consistently fall below model calculations by more than 15% for ozone column depletion. The very large departures of EER irradiance in pollution episodes suggests that

much of the additional depletion of EER irradiance is due to local sources of anthropogenic pollutants. Bais et al. (1996) find that summer values of EER dose at Kos, an island in the eastern Aegean, average 15% greater than at Athens although the difference in latitude of these stations can account for less than 1% difference in incoming solar radiation at these sites. Differences in EER dose of this magnitude could be explained by a systematic differences in cloud cover as well as variation in concentration of tropospheric pollutants across the Aegean.

The problems with the detection of associated secular trends in UV and total ozone are illustrated by a comparison of the daily time series of EER irradiance at constant solar zenith angle of 63° and for column ozone for a three year period (Fig. 9). Both the day to day variation and the annual variation

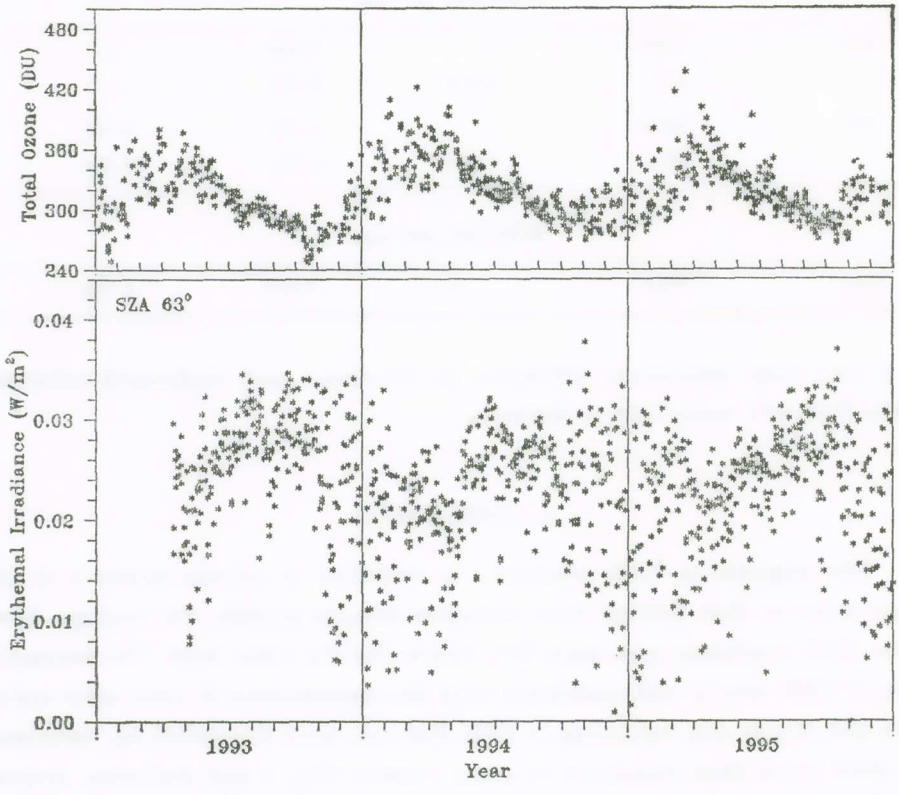

Fig. 9. Time series of daily values of column ozone (upper panel) and of EER irradiance (reduced to the mean earth-sun distance) at constant SZA = 63° (lower panel) for the period 1993-1995.

of ozone are driven by fluctuations in stratospheric circulation which have a large interannual and spatial variability at mid and polar latitudes. Theocaris et al. (1996) presented a review of six years of observations of UV irradiance at 305 nm and total ozone at Thessaloniki one of the longest records of concurrent observations that is available. Monthly averages of total ozone and UV irradiance for cases of cloud cover less than 3/8 showed satisfactory coherence. Because of the large interannual variability, however, ozone trends derived from these sata were highly dependent on the selection of time interval for the calculation. Global and long term fluctuations in total ozone are difficult to establish since satellite observations only span a few decades and are plagued by drifts in instrumental calibration and the spatial coverage of ground based stations is limited. It is of some significance, therefore, that a decadal signal of global dimension can be detected (Zerefos et al., 1997). These oscillations have a peak to peak amplitude of a few per cent and are approximately in phase with the 11 year cycle of solar activity. A UV fluctuation of similar magnitude can be anticipated[1].

ACKNOWLEDGEMENTS

This project was supported by the Research Committee of the Academy of Athens and by the General Secretariat for Research and Technology of the Ministry of Industry, Energy and Technology (project STRIDE HELLAS 326). Thanks are expressed to Institute of Meteorology and Atmospheric Environment of National Observatory of Athens for providing unpublished meteorological data.

REFERENCES

Ambach W. and M. Blumthaler, Characteristics of solar UV irradiance, *Meteorol. Zeitschrift*, N.F. 3, 211-220, 1994.

Bais A., C. Meleti, C. Zerefos and C. Repapis, Solar UV radiation in Greece,

1. The fluctuation in solar output which is assumed to be responsible for the decadal ozone variation is confined to the less than 120 mm UV wavelengths that are absorbed in the upper stratosphere. The magnitude of the variation in the UVB band during high solar activity is less than 1% (Brasseur, 1993).

Proc. 3rd Greek Meeting on Meteorology, Climatology, Atmospheric Physics, Athens 25-27 Sep. 1996, 396-401, 1996.

Brasseur G., The Response of the Middle Atmosphere to Long-Term and Short-Term Solar Variability: A Two Dimensional Model, *J. Geophys. Res.* 98, 23079-23090, 1993.

Forster P. M. de F., Modeling ultraviolet radiation at the earth's surface. Part I: The sensitivity of ultraviolet irradiances to atmospheric changes, *J. Appl. Meteor.* 34, 2412-2425, 1995.

Forster P. M. de F., K. P. Shine and A. R. Webb, Modeling ultraviolet radiation at the earth's surface Part II: model and instrument comparison *J. Appl. Meteor.*, 34, 2426-2439, 1995.

Gardiner B. G., A. R. Webb, A. F. Bai, M. Blumthaler, I. Dirmhirn, P. Forster, D. Gillotay, K. Henriksen, M. Huber, P. J. Kirsch, P. C. Simon, T. Svenoe, P. Weihs and C. S. Zerefos, European intercomparison of ultraviolet spectroradiometers, *Environmental Technology*, 14, 25-43, 1993.

Green A. E. S., T. Mo and J. H. Miller, A study of solar erythema radiation doses, *Photochem. Photobiol..*, 20, 473, 1974.

Madronich S. L., Changes in biologicaly damaging ultraviolet (UV) radiation: Effect of overhead ozone and cloud amount, *Report of effects of solar ultraviolet radiation on Geochemical Dynamics in Aquatic Environments Workshop*, Edited by N. B. Blong and R. G. Zepp, 30-31, 1989.

Mantis H., C. Repapis, C. Zerefos and J. Ziomas, Assesment of the potential for photochemical air polution in Athens: A Comparison of emissions and air pollutant levels in Athens with those in Los Angeles, *J. Appl. Meteor.*, 31, 1467-1476, 1992.

McKenzie R. L., W. A. Matthews and P. V. Johnston, The relationship between erythemal UV and ozone, derived from spectral irradiance measurements, *Geophys. Res. Let.*, 18, 2269-2272, 1991.

McKinlay A., and B. L. Diffey, A reference action spectrum for ultraviolet induced erythema in human skin, in W. F. Passchier and B. F. M. Bosnjakovic (eds), *Human exposure to ultraviolet radiation: Risks and regulations, Elsevier Science*, 83-87, 1987.

McKinlay A. F. and B. L. Diffey, A reference action spectrum for ultraviolet induced erythema in human skin. *Commission internationale de l'Eclairage* (CIE), - J. 6, 17-22, 1987.

National Observatory of Athens, *Climatological Bulletin*, Athens, Greece.

Ozone Data for the World (Atmospheric Environment Service, Department of the Environment Downsview, Ontario, Canada, in cooperation with the World Meteorological Organization).

Prasad B. S. N., H. B. Gayathi, N. Muralikrishnan and B. N. Murthy, Seasonal variation of global UV-B flux and its dependence on atmospheric ozone and particulate at a low latitude station, *Tellus*, 44B, 237-242, 1992.

Theocaris P., C. Zerefos, A. Bais and C. Meleti, Variability of Ozone and Solar Ultraviolet Radiation in Greece. Proc. Academy of Athens, 1996.

Zerefos C., K. Tourpali, B. R. Bojkov, D. S. Balis, B. Rognerund and I. S. A. Isaksen, Solar Activity - Total Column Relationships: Observations and Model Studies with Heterogeneous Chemistry, *J. Geophys. Res.*, 102, 1561-1569, 1997.

Ziomas J., Mediterranean Campaign of Photochemical Tracers Transport and Chemical evolution (MEDCAPHOT). An overview, submitted to *Atmospheric Environment*, 1997.

ΠΕΡΙΛΗΨΗ

Κλιματολογία τῆς ἡλιακῆς ὑπεριώδους ἀκτινοβολίας στὴν Ἀθήνα

Στὴν παροῦσα ἔρευνα μελετήθηκαν γιὰ τὴν περιοχὴ τῶν Ἀθηνῶν οἱ μεταβολὲς τῆς ὑπεριώδους ἡλιακῆς ἀκτινοβολίας, στὴν περιοχὴ τοῦ φάσματος 280-320 nm (UVB), ποὺ φθάνει στὴν ἐπιφάνεια τῆς γῆς, γιὰ τὴν περίοδο ἀπὸ 13 Ἀπριλίου 1993 31 Δεκεμβρίου 1995.

Ἡ UVB ἀκτινοβολία ἡ ὁποία ἀντιπροσωπεύει μόλις τὸ 1.7% τῆς ἐνεργείας τῆς ἡλιακῆς ἀκτινοβολίας ποὺ φθάνει στὸ ἀνώτατο ὅριο τῆς ἀτμόσφαιρας (ἡλιακὴ σταθερά, 1367 Wm^{-2}) ἀπορροφᾶται μερικῶς ἀπὸ τὸ ὄζον καὶ μόνο ἀκτινοβολία μὲ μήκη κύματος μεγαλύτερα ἀπὸ 290 nm παρατηρεῖται στὸ ἔδαφος. Ἐκτὸς ἀπὸ τὴν ἀπορρόφηση ἀπὸ τὸ ὄζον ἡ UVB ἡλιακὴ ἀκτινοβολία σκεδάζεται ἀπὸ τὰ νέφη, τὰ μόρια διαφόρων ἀερίων ρύπων καὶ τὰ ἀερολύματα μὲ ἀποτέλεσμα ἡ ἐξασθένηση τῆς UV-B ἀκτινοβολίας ποὺ φθάνει στὸ ἔδαφος νὰ ἀνέρχεται γενικῶς σὲ 75% ἢ καὶ μέχρι σχεδὸν 100% σὲ περιπτώσεις πλήρους νεφοκαλύψεως ἀπὸ μεγάλα πυκνὰ νέφη. Οἱ ζωντανοὶ ὀργανισμοὶ εἶναι λίαν εὐαίσθητοι στὴν UVB ἀκτινοβολία.

Ἡ παρατηρουμένη τάση μειώσεως τοῦ στρατοσφαιρικοῦ ὄζοντος κατὰ τὰ τελευταῖα ἔτη ἀναμένεται νὰ προκαλέσει αὔξηση τῆς ὑπεριώδους ἡλιακῆς ἀκτινοβολίας UVB ποὺ φθάνει στὴν ἐπιφάνεια τῆς γῆς, μὲ βλαβερὲς γιὰ τὰ ἔμβια ὄντα συνέπειες. Ἡ ἀνίχνευση ὅμως σημαντικῆς μεταβολῆς στὰ ἐπίπεδα τῆς UV ἀπαιτεῖ μακροχρόνιες ἀκριβεῖς μετρήσεις καὶ σὲ διάφορα κλιματικὰ καθεστῶτα. Ἐπίσης εἶναι γνωστὸ ὅτι ἡ ἠλεκτρομαγνητικὴ ροὴ ἀπὸ τὸν ἥλιο δὲν εἶναι τελείως σταθερὰ ἀλλὰ μεταβάλλεται ἐλαφρῶς, ἰδιαίτερα στὰ μικρὰ μήκη κύματος. Στὴν UVB ὅμως περιοχὴ τοῦ φάσματος καὶ ἰδιαίτερα στὴν περιοχὴ 282-303 nm ἡ μεταβολή, ἀπὸ τὸ ἡλιακὸ μέγιστο στὸ ἡλιακὸ ἐλάχιστο τῆς ἑνδεκαετοῦς μεταβολῆς τῆς ἡλιακῆς δραστηριότητας, ὑπολογίζεται ὅτι εἶναι $< 1\%$.

Ἐρύθημα τοῦ ἐκτιθεμένου στὸν ἥλιο ἀνθρωπίνου δέρματος προκαλοῦν οἱ ἀκτινοβολίες ποὺ ἀνήκουν στὴν φασματικὴ περιοχὴ μὲ μήκη κύματος 280-400 nm(UV).

Ἡ δραστικότητα ὅμως τῆς ἀκτινοβολίας μεταβάλλεται μὲ τὸ μῆκος κύματος. Ἡ συνολικὴ ἐνέργεια τῆς ἡλιακῆς ἀκτινοβολίας ποὺ ἀνήκει στὴ φασματικὴ αὐτὴ περιοχή, βεβαρυμένη μὲ τὸ φάσμα δραστικότητος (action spectrum) τῆς ὑπεριώδους ἡλιακῆς ἀκτινοβολίας γιὰ τὴν πρόκληση ἐρυθήματος στὸ ἀνθρώπινο δέρμα, καλεῖται «ἐρυθηματώδης δόση» (erythemal dose). Τὸ διεθνῶς ἀποδεκτὸ σήμερα φάσμα δραστικότητος εἶναι τὸ «CIE (Commission Internationale d'Eclairage) erythemal action spectrum» ὅπως καθορίσθηκε ἀπὸ τοὺς Mckinlay καὶ Diffey (1987).

Στὰ πλαίσια συνεργασίας μὲ τὸ Ἐργαστήριο Φυσικῆς τῆς Ἀτμοσφαίρας τοῦ Ἀριστοτελείου Πανεπιστημίου Θεσσαλονίκης σὲ πρόγραμμα μετρήσεων καὶ μελέτης τῆς ἡλιακῆς UVB, ἐγκαταστήσαμε στὴ στέγη τῆς πολυκατοικίας ποὺ στεγάζεται τὸ Κέντρο Ἐρεύνης Φυσικῆς τῆς Ἀτμοσφαίρας καὶ Κλιματολογίας τῆς Ἀκαδημίας Ἀθηνῶν ἕνα ἀκτινόμετρο συνεχοῦς καταγραφῆς τύπου UVB-1 τῆς Yankee Environmental Systems (YES). Τὰ ἀκτινόμετρα αὐτὰ ἔχουν συνάρτηση φασματικῆς ἀποκρίσεως ποὺ σχεδὸν συμπίπτει μὲ τὴν ἐρυθηματώδη φσματικὴ ἀπόκριση.

Οἱ παράγοντες ποὺ ἐπηρεάζουν τὴν ὑπεριώδη ἡλιακὴ ἀκτινοβολία UV-B καὶ ὡς ἐκ τούτου τὴν ἐρυθηματώδη δόση εἶναι ἡ ζενιθία γωνία τοῦ ἡλίου, τὸ ὁλικὸ ποσὸ τοῦ ὄζοντος τῆς ἀτμοσφαίρας, τὰ νέφη, τὰ ἀερολύματα καὶ οἱ ἀέριοι ρῦποι. Ἡ ἐτήσια πορεία τῶν ἡμερησίων τιμῶν τῆς ἐρυθηματώδους δόσεως (Erythemal effective radiation, EER ὅπως ἔχει ὁρισθεῖ) φανερώνει τὴ μεγάλη ἐτήσια μεταβολή της ποὺ παρακολουθεῖ τὴν ἐτήσια μεταβολὴ τῆς ζενιθίας γωνίας τοῦ ἡλίου. Ἡ σχετικὴ ὅμως μεταβολὴ τῆς EER ἀπὸ τὸν χειμώνα στὸ θέρος εἶναι τριπλασία τῆς ἀντίστοιχης μεταβολῆς τῆς ὁλικῆς ἡλιακῆς ἀκτινοβολίας στὰ μέσα γεωγραφικὰ πλάτη.

Ἡ ἐτησία πορεία τοῦ ὁλικοῦ ὄζοντος (τοῦ ὄζοντος ποὺ περιέχεται στὴ στήλη ἀπὸ τὴν ἐπιφάνεια τοῦ ἐδάφους μέχρι τὸ ὅριο τῆς ἀτμόσφαιρας) στὰ μέσα γεωγραφικὰ πλάτη παρουσιάζει ἕνα μέγιστο τὴν ἄνοιξη καὶ ἕνα ἐλάχιστο τὸ τέλος τοῦ φθινοπώρου. Οἱ ἡμερήσιες τιμὲς τοῦ ὁλικοῦ ὄζοντος παρουσιάζουν μεγάλη διακύμανση ἀπὸ ἡμέρα σὲ ἡμέρα. Διὰ τὴν περίπτωση τῶν τιμῶν τοῦ 1994 διὰ τὴν Ἀθήνα ἡ βελτίστης προσαρμογῆς πολυωνυμικὴ 3ου βαθμοῦ καμπύλη, ἡ ὁποία ἀπὸ τὸ μέγιστο (τὸν Ἀπρίλιο) μέχρι τὸ ἐλάχιστο (τὸν Νοέμβριο) ἔχει εὖρος περίπου 64 DU (20% τῆς μέσης ἐτησίας τιμῆς), ἑρμηνεύει μόλις τὸ 30% τῆς διακυμάνσεως τῶν ἡμερησίων τιμῶν.

Διὰ τὴν ἐκτίμηση τῶν ἀναμενομένων τιμῶν τῆς ἐρυθηματώδους δόσεως χρησιποιήθηκαν δύο πρότυπα (μοντέλα) διαδόσεως ἀκτινοβολίας (radiative transfer models) στὴν ἀτμόσφαιρα. Οἱ μεταβολὲς τῆς παρατηρουμένης ἐρυθηματώδους ἀκτινοβολίας (EER) λόγω τῶν μεταβολῶν τοῦ ὁλικοῦ ὄζοντος εἶναι τῆς ἰδίας τάξεως μεγέθους μὲ αὐτὲς ποὺ προκύπτουν ἀπὸ τὰ μοντέλα διαδόσεως τῆς ἡλιακῆς ἀκτινοβο

λίας στὴν ἀτμόσφαιρα, ὅμως ἡ μετρουμένη EER εἶναι κατὰ μέσο ὅρο μικρότερη κατὰ τουλάχιστο 20% τῆς ὑπολογιζομένης διὰ ἀνέφελο οὐρανό.

Ἡ ὁλικὴ ἡλιακὴ ἀκτινοβολία ποὺ φθάνει στὸ ἔδαφος, στὴν περιοχὴ τῶν Ἀθηνῶν, εἶναι περίπου κατὰ 25% (θέρος) ἕως 35% (χειμώνα) λιγότερη ἀπὸ τὴν ἀντίστοιχη ποὺ προσπίπτει στὸ ὅριο τῆς ἀτμόσφαιρας, λόγω μοριακῆς ἀπορροφήσεως καὶ σκεδάσεως στὴν ἀτμόσφαιρα καὶ λόγω τῶν νεφῶν. Τὰ νέφη, ἰδιαίτερα τὸν χειμώνα, μποροῦν νὰ ἐξασθενήσουν ἐπιπλέον τὴν ὁλικὴ ἡλιακὴ ἀκτινοβολία κατὰ περίπου 60%. Τὸ ποσοστὸ τῆς μετρουμένης στὸ ἔδαφος ἐρυθηματώδους δόσεως ὡς πρὸς τὴν ὑπολογιζομένη ἀπὸ τὰ μοντέλα διὰ τὸ ἴδιο ποσὸ ὄζοντος, συσχετίζεται πολὺ καλὰ μὲ τὸ ποσοστὸ τῆς ὁλικῆς ἡλιακῆς ἀκτινοβολίας ποὺ φθάνει στὸ ἔδαφος (πηλίκο τῆς μετρουμένης ὁλικῆς ἡλιακῆς ἀκτινοβολίας πρὸς τὴν ὑπολογιζομένη προσπίπτουσα στὸ ὅριο τῆς ἀτμόσφαιρας). Ἡ σχέση αὐτὴ δείχνει τὴν μεγάλη ἐπίδραση στὴν ἐξασθένηση τῆς UV καὶ ἄλλων ἐκτὸς τοῦ ὄζοντος παραγόντων. Οἱ ἀπὸ ἡμέρα σὲ ἡμέρα μεταβολὲς τῆς ἐρυθηματώδους δόσεως ἐξαρτῶνται, κυρίως κατὰ τὴν ψυχρὴ περίοδο τοῦ ἔτους, περισσότερο ἀπὸ τὶς μεταβολὲς τῆς νεφοκαλύψεως ἀπὸ ὅτι ἀπὸ τὶς μεταβολὲς τοῦ ὄζοντος. Τὸ θέρος οἱ τιμὲς τῆς EER ἀκόμα καὶ ὑπὸ ἀνέφελο οὐρανὸ εἶναι κατὰ 15% μικρότερες ἀπὸ ὅτι οἱ λόγω μειώσεως τοῦ ὄζοντος ὑπολογιζόμενες ἀπὸ τὰ μοντέλα τιμὲς τῆς EER. Ἐξ ἄλλου οἱ μεγάλες ἀποκλίσεις τῆς ἐρυθηματώδους ἀκτινοβολίας κατὰ τὴν διάρκεια ἐπεισοδίων ρυπάνσεως φανερώνουν ὅτι μεγάλο ποσοστὸ τῆς ἐπιπλέον ἐξασθενήσεως τῆς ἐρυθηματώδους ἀκτινοβολίας ὀφείλεται σὲ τοπικὲς πηγὲς ρύπων ἀνθρωπογενοῦς προελεύσεως.

Οἱ χρονοσειρὲς τῶν ἡμερησίων τιμῶν τῆς ἐρυθηματώδους ἀκτινοβολίας, γιὰ μία δεδομένη ζενιθία γωνία ἡλίου, συγκρινόμενες μὲ τὶς ἀντίστοιχες τοῦ ὄζοντος φανερώνουν ὅτι οἱ μέγιστες τιμὲς τῆς ἀκτινοβολίας ἐμφανίζονται κατὰ τὴν ἐποχὴ τοῦ ἐλαχίστου τοῦ ὄζοντος. Ὅμως, οἱ ἐπὶ τοῖς ἑκατὸ διακυμάνσεις τῆς ἐρυθηματώδους ἀκτινοβολίας εἶναι κατὰ πολὺ μεγαλύτερες ἀπὸ τὶς ἀντίστοιχες τοῦ ὄζοντος, λόγω μεγάλης ἐξασθενήσεως τῆς UV ἀκτινοβολίας καὶ ἀπὸ ἄλλους παράγοντες.

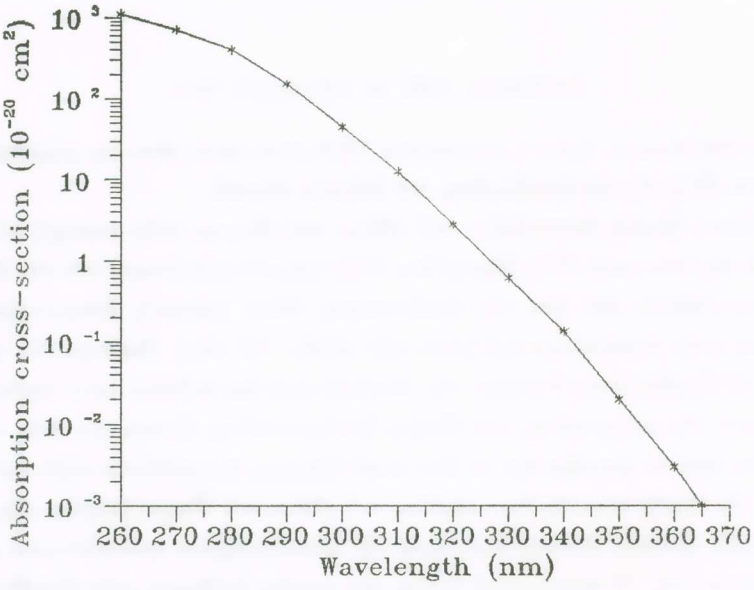

Fig. A1. Ozone absorption cross-section per molecule in cm².

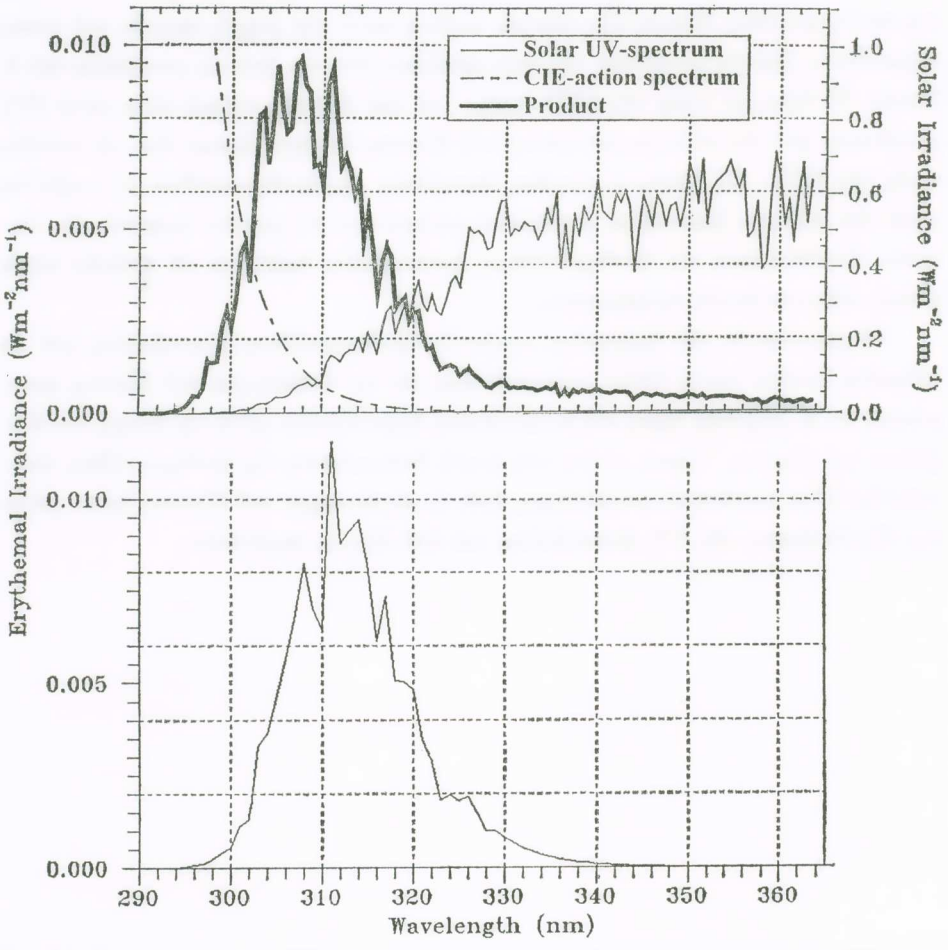

Fig. A2. Upper panel: the CEI-action spectrum (dashed line), a measured solar UV-spectrum (solid line), and the product of the two (erythemal irradiance, heavy line). (From Kuik and Kelder, 1994). Lower panel: the product of the response function of the YES UVB-1 pyranometer with the measured solar UV-spectrum of the upper panel.

APPENDIX B

STATISTICS: OZONE, ERYTHEMAL DOSE

		O_3 (DU)			EER (KJ /m^2·day)		
		mean	st dev	No	mean	st dev	No
1993	J	296	27.94	24			
	F	317	30.01	16			
	M	332	23.43	19			
	A	332	19.01	21	3.125	0.416	15
	M	341	18.67	18	2.984	1.029	31
	J	328	13.64	19	3.919	0.665	30
	J	302	9.89	28	4.232	0.494	31
	A	299	6.82	27	3.661	0.633	31
	S	288	6.48	26	2.686	0.340	30
	O	275	16.57	28	1.538	0.338	29
	N	278	9.99	13	0.604	0.325	30
	D	298	21.49	21	0.470	0.111	31
	Y	305	27.15	260			
1994	J	326	26.91	16	0.528	0.167	31
	F	357	27.50	16	0.767	0.309	21
	M	355	24.24	27	1.651	0.536	31
	A	355	19.70	22	2.437	0.689	30
	M	349	21.02	25	3.306	0.942	29
	J	330	17.74	29	4.097	0.793	30
	J	320	12.72	31	3.871	0.549	31
	A	311	11.36	31	3.353	0.425	31
	S	299	10.18	29	2.367	0.500	28
	O	292	9.63	25	1.241	0.368	30
	N	292	15.04	23	0.662	0.246	30
	D	301	18.64	23	0.403	0.142	31
	Y	323	29.53	297	2.083	1.411	353
1995	J	304	22.48	22	0.527	0.250	31
	F	315	23.74	21	1.038	0.355	28
	M	343	35.37	21	1.663	0.557	31
	A	350	24.26	24	2.411	0.716	30
	M	340	10.99	28	3.348	0.675	31
	J	321	24.26	30	3.929	0.506	30
	J	317	17.45	31	3.787	0.571	30
	A	301	9.18	31	3.216	0.599	31
	S	291	12.12	26	2.457	0.674	30
	O	288	14.67	27	1.413	0.505	31
	N	309	17.69	18	0.606	0.239	23
	D	312	18.38	12	0.367	0.128	31
	Y	316	27.07	291	2.093	1.345	357

STATISTICS: ERYTHEMAL IRRADIANCE (W/m²)

MORNING

		63°			45°			30°		
		mean	st dev	No	mean	st dev	No	mean	st dev	No
1993	J									
	F									
	M									
	A	0.0263	0.0044	15	0.0807	0.0172	15	0.1256	0.0204	15
	M	0.0231	0.0065	31	0.0677	0.0245	31	0.0989	0.0338	31
	J	0.0270	0.0043	30	0.0811	0.0184	30	0.1122	0.0230	30
	J	0.0297	0.0039	31	0.0952	0.0106	31	0.1344	0.0147	31
	A	0.0295	0.0060	31	0.0947	0.0119	31	0.1322	0.0198	31
	S	0.0315	0.0039	30	0.0953	0.0126	21			
	O	0.0318	0.0045	29						
	N	0.0237	0.0093	30						
	D	0.0247	0.0066	31						
	Y									
1994	J	0.0221	0.0080	22						
	F	0.0216	0.0064	21						
	M	0.0227	0.0063	31	0.0768	0.0236	11			
	A	0.0197	0.0060	30	0.0678	0.0189	30	0.0921	0.0282	21
	M	0.0231	0.0042	30	0.0737	0.0173	30	0.1072	0.0313	31
	J	0.0258	0.0054	30	0.0850	0.0136	30	0.1210	0.0190	30
	J	0.0260	0.0025	31	0.0847	0.0110	31	0.1210	0.0179	31
	A	0.0263	0.0030	31	0.0878	0.0083	31	0.1234	0.0173	31
	S	0.0263	0.0038	28	0.0862	0.0120	19			
	O	0.0259	0.0071	30						
	N	0.0259	0.0097	30						
	D	0.0227	0.0089	31						
	Y	0.0241	0.0066	345						
1995	J	0.0224	0.0101	22						
	F	0.0265	0.0069	28						
	M	0.0210	0.0094	31	0.0710	0.0218	11			
	A	0.0208	0.0052	30	0.0704	0.0203	30	0.0817	0.0425	21
	M	0.0223	0.0052	31	0.0724	0.0170	31	0.1083	0.0262	31
	J	0.0262	0.0030	30	0.0809	0.0102	30	0.1158	0.0141	30
	J	0.0260	0.0055	31	0.0856	0.0102	31	0.1204	0.0179	31
	A	0.0307	0.0038	31	0.0908	0.0139	31	0.1258	0.0227	31
	S	0.0309	0.0071	30	0.0980	0.0127	21			
	O	0.0280	0.0066	31						
	N	0.0232	0.0090	23						
	D	0.0201	0.0096	31						
	Y	0.0249	0.0078	349						

STATISTICS: ERYTHEMAL IRRADIANCE (W/m²)

EVENING

		63°			45°			30°		
		mean	st dev	No	mean	st dev	No	mean	st dev	No
1993	J									
	F									
	M									
	A	0.0208	0.0042	15	0.0764	0.0104	15	0.1170	0.0209	15
	M	0.0176	0.0071	31	0.0595	0.0277	31	0.0829	0.0400	31
	J	0.0216	0.0049	30	0.0757	0.0161	30	0.1095	0.0246	30
	J	0.0244	0.0039	31	0.0820	0.0116	31	0.1171	0.0237	31
	A	0.0249	0.0036	31	0.0860	0.0140	31	0.1255	0.0200	31
	S	0.0266	0.0045	30	0.0909	0.0104	19			
	O	0.0253	0.0049	29						
	N	0.0183	0.0093	30						
	D	0.0243	0.0087	31						
	Y									
1994	J	0.0208	0.0085	28						
	F	0.0180	0.0087	22						
	M	0.0179	0.0049	31	0.0662	0.0268	11			
	A	0.0177	0.0061	30	0.0623	0.0220	30	0.0978	0.0267	22
	M	0.0180	0.0068	30	0.0635	0.0271	30	0.0978	0.0338	31
	J	0.0243	0.0042	30	0.0802	0.0177	30	0.1124	0.0331	30
	J	0.0231	0.0066	31	0.0739	0.0232	31	0.1063	0.0349	31
	A	0.0232	0.0041	31	0.0814	0.0078	31	0.1184	0.0180	31
	S	0.0229	0.0033	29	0.0849	0.0107	18			
	O	0.0212	0.0071	30						
	N	0.0219	0.0081	30						
	D	0.0200	0.0099	31						
	Y	0.0208	0.0070	353						
1995	J	0.0199	0.0112	28						
	F	0.0199	0.0074	28						
	M	0.0204	0.0064	31	0.0755	0.0166	11			
	A	0.0178	0.0055	30	0.0604	0.0221	30	0.0834	0.0421	22
	M	0.0186	0.0058	31	0.0678	0.0201	31	0.0999	0.0273	31
	J	0.0206	0.0059	30	0.0751	0.0160	30	0.1110	0.0233	30
	J	0.0214	0.0052	31	0.0709	0.0198	31	0.1060	0.025	30
	A	0.0216	0.0035	31	0.0695	0.0224	31	0.1037	0.0363	31
	S	0.0198	0.0064	30	0.0852	0.0159	19			
	O	0.0249	0.0064	31						
	N	0.0207	0.0073	24						
	D	0.0178	0.0071	31						
	Y	0.0203	0.0068	356						